5872–5881 *Nucleic Acids Research, 2008, Vol. 36, No. 18* *Published online 16 September 2008*
doi:10.1093/nar/gkn592

Cosegregation of novel mitochondrial 16S rRNA gene mutations with the age-associated T414G variant in human cybrids

Peter Seibel[1,*], Chiara Di Nunno[2], Christian Kukat[1], Ingo Schäfer[1], Roberto Del Bo[3], Andreina Bordoni[3], Giacomo P. Comi[3], Astrid Schön[1], Ferdinando Capuano[2], Dominga Latorre[2] and Gaetano Villani[2]

[1]Department of Molecular Cell Therapy, Center for Biotechnology and Biomedicine, Universität Leipzig, Deutscher Platz 5, 04103 Leipzig, Germany, [2]Department of Medical Biochemistry, Biology & Physics, University of Bari, Piazza Giulio Cesare, 11, 70124 - Bari, Italy and [3]Dino Ferrari Center, Foundation IRCCS Ospedale Maggiore Policlinico, Mangiagalli and Regina Elena, Department of Neurological Sciences, University of Milano, Via Sforza, 35, 20122 - Milano, Italy

Received June 11, 2008; Revised August 13, 2008; Accepted September 3, 2008

ABSTRACT

Ever increasing evidence has been provided on the accumulation of mutations in the mitochondrial DNA (mtDNA) during the aging process. However, the lack of direct functional consequences of the mutant mtDNA load on the mitochondria-dependent cell metabolism has raised many questions on the physiological importance of the age-related mtDNA variations. In the present work, we have analyzed the bioenergetic properties associated with the age-related T414G mutation of the mtDNA control region in transmitochondrial cybrids. The results show that the T414G mutation does not cause *per se* any detectable bioenergetic change. Moreover, three mtDNA mutations clustered in the 16S ribosomal RNA gene cosegregated together with the T414G in the same cybrid cell line. Two of them, namely T1843C and A1940G, are novel and associate with a negative bioenergetic phenotype. The results are discussed in the more general context of the complex heterogeneity and the dramatic instability of the mitochondrial genome during cell culture of transmitochondrial cybrids.

INTRODUCTION

Human mitochondria are known as the power plants of eukaryotic cells. To fulfil their main task, they utilize reduction equivalents in form of NADH and molecular oxygen to generate an electrochemical potential across the inner mitochondrial membrane that is in turn utilized to generate ATP. Deficiencies in oxidative phosphorylation (OxPhoS) activity ultimately lead to a decrease in oxidative energy supply. Moreover, OxPhoS defects are accompanied by an increase of reactive oxygen species. The reactive oxygen species come into play when electrons in the initial steps of the malfunctioning electron transport chain are transferred directly to molecular oxygen. The formed superoxide anion (O_2^-) is converted by the mitochondrial superoxide dismutase to hydrogen peroxide (H_2O_2) that can further generate a number of other reactive oxygen/nitrogen species, thereby damaging membranes, proteins, RNA and DNA.

Ever increasing evidence has been accumulated in the recent years on the role played by the mitochondria during the aging process (1,2). In particular, attention has been paid to the characterization and identification of age-associated mitochondrial DNA (mtDNA) mutations (3). Rearrangements of mtDNA molecules have been usually found at very low levels, thus questioning their functional significance (3). However, recent reports have demonstrated that high levels of mtDNA deletions can be detected in substantia nigra neurons in aging (4,5).

Moreover, the work of Michikawa *et al*. (6) showed that specific single base replacements of mtDNA can accumulate during aging in human fibroblasts and opened a complete new aspect in this field. This work was further substantiated by animal models that focused on the premature aging in mice expressing defective mtDNA polymerase gamma (7). Also in this case, the contribution of mtDNA point mutations to the aging process has been recently challenged (8). Therefore, the physiological importance of mtDNA variations is still under intense debate (9).

The aim of the present work was to study the functional impact of the age-related T414G mutation that is located

*To whom correspondence should be addressed. Tel: +49 341 9731370; Fax: +49 341 9731379; Email: peter.seibel@bbz.uni-leipzig.de
Correspondence may also be addressed to Gaetano Villani, Tel: +39 080 5448534; Fax: +39 080 5448538; Email: villani@biochem.uniba.it

in the mtDNA control region (6). In order to minimize the influence of nuclear/mitochondrial genome background, we have first analyzed the biochemical phenotype of homoplasmic transmitochondrial cybrids carrying either the 414T (wild-type) or 414G (mutant) mtDNA genotype deriving from the same heteroplasmic mitochondrial donor(s) and nuclear acceptor cell lines. Our results show that the T414G mutation does not cause *per se* any detectable bioenergetic change. Unexpectedly, when we checked the complete mtDNA sequence of the only homoplasmic T414G cybrid (AL4.3) showing a negative bioenergetic phenotype, we found three additional mutations in the 16S rRNA gene. Two of these mutations were responsible for a defective mitochondrial protein synthesis efficiency.

The results are finally discussed in the larger context of the suitability of the transmitochondrial cybrid system for the characterization of the phenotypic impact of specific mtDNA alterations.

MATERIALS AND METHODS

Cell lines and media

The AL4.3, AL4.5, 1AC1.2 human cell lines, carrying in homoplasmic form the T414G transversion in the mtDNA and the AL4.8, AL4.27 and 1AC1.48 cell lines, carrying in homoplasmic form the wild-type version (T) of the same position (414) of the mtDNA, were previously isolated by transfer into human mtDNA-less 143B.TK$^-$ $\rho^0$206 cells of mitochondria from fibroblasts of the individuals 100-3y (for the AL series of transformants) and 98y (for the 1AC series of transformants) (6,10). All cell lines were grown in DMEM, supplemented with 10% fetal bovine serum (FBS). The $\rho^0$206 cell line was grown in DMEM with 10% FBS and 50 μg/ml uridine. For growth measurements in selective galactose medium, cells were cultured in DMEM lacking glucose and containing 0.9 mg of galactose/ml and 0.5 mg of pyruvate/ml supplemented with 10% dialyzed FBS.

Measurement of respiration rates in intact cells

The respiratory activity of intact cells was measured polarographically with a Clark-type oxygen electrode in a water-jacketed chamber (Hansatech Instruments, Norfolk, UK), magnetically stirred at 37°C, as previously described (11,12). Briefly, exponentially growing cells, fluid changed the day before the measurement, were collected by trypsinization and centrifugation, and then transferred into the polarographic chamber at $3–4 \times 10^6$ cells/ml in TD Buffer (0.137 M NaCl, 5 mM KCl, 0.7 mM Na_2HPO_4, 25 mM Tris–HCl, pH 7.4), previously air equilibrated at 37°C. The resuspended cell samples were read directly (basal endogenous respiration) and after addition of 2,4-dinitrophenol (DNP) to 25–30 μM (uncoupled endogenous respiration) or of DNP, antimycin A (20 nM), TMPD (Fluka/Sigma-Aldrich Chemie GmbH, Buchs SG, Switzerland) (0.4 mM) and sodium ascorbate (10 mM) (cellular cytochrome oxidase respiratory activity).

Determination of mitochondrial enzyme activities

Cells, collected by trypsinization and centrifugation, were resuspended in buffer A (75 mM sucrose, 5 mM KH_2PO_4, 40 mM KCl, 0.5 mM EDTA, 3 mM $MgCl_2$, 30 mM Tris–HCl, pH 7.4), counted and supplemented with 15–20 μg/10^6 cells of digitonin. After 1–2 min, the cell suspension was further diluted by adding nine volumes of the same buffer supplemented with 0.3% fatty-acid-free bovine serum albumin and centrifuged; the pellet was then resuspended in hypotonic medium (25 mM potassium phosphate, pH 7.4, 5 mM $MgCl_2$), supplemented with antiproteases cocktail (Roche Diagnostics, Mannheim, Germany). In order to allow complete accessibility of substrates to the inner mitochondrial membrane enzymes, samples were freeze-thawed three times. All enzyme activities were measured at 30°C using 0.1–0.3 mg/ml of lysate proteins with a Beckman DU7400 spectrophotometer equipped with a rapid-mixing apparatus, as previously described (13).

NADH–CoQ oxidoreductase (Complex I) activity was measured in hypotonic medium supplemented with fatty-acid-free bovine serum albumin (BSA) (2.5 mg/ml) in the presence of 2 mM KCN, antimycin A (2 μg/ml) and 65 μM decylubiquinone, by following the rotenone-sensitive initial rate of NADH (13 mM) oxidation at 340–425 nm ($\Delta\varepsilon = 6.81\ mM^{-1}\ cm^{-1}$). Rotenone (2 μg/ml) inhibited the enzymatic activity by 85–95%.

Succinate dehydrogenase (Complex II) activity was measured in hypotonic medium in the presence of succinate (20 mM), rotenone (2 μg/ml), antimycin (2 μg/ml) and 2,6-dichlorophenolindophenol (50 μM) by following the reduction of 2,6-dichlorophenolindophenol at 600 nm ($\varepsilon = 19.1\ mM^{-1}\ cm^{-1}$). Prior to the measurement, proteins were incubated for 10 min in the hypotonic medium in the presence of 20 mM succinate. The reaction was started with decylubiquinone (65 μM). The sensitivity of the reaction to the complex II inhibitor malonate (20 mM) was of 98%.

Succinate–cytochrome c oxidoreductase (complex II + III) activity was measured at 550–540 nm ($\Delta\varepsilon = 19.1\ mM^{-1}\ cm^{-1}$) as initial rate of antimycin-sensitive cytochrome c reduction. As for complex II assay, a preincubation of proteins for 10 min in the assay buffer plus succinate (20 mM) was required. Rotenone (3 μg/ml), 2 mM KCN and 65 μM decylubiquinone were added to the assay buffer and after baseline recording, the reaction was started by the addition of 20 μM ferricytochrome c. The activity was 90–95% inhibited by antimycin A (2 μg/ml).

Cytochrome c oxidase (complex IV) activity was measured by following the oxidation of ferrocytochrome c (20 μM) at 550–540 nm ($\Delta\varepsilon = 19.1\ mM^{-1}\ cm^{-1}$). Enzymatic activity was estimated in the assay buffer supplemented with 0.5 mM dodecyl maltoside in the presence of antimycin A (3 μg/ml), as the apparent first-order rate constant after all cytochrome c oxidation induced by the addition of few grains of potassium hexacyanoferrate. This rate was inhibited over 95% by KCN (2 mM).

Citrate synthase activity, used as mitochondrial matrix enzymatic marker, was measured in hypotonic medium plus 0.3 mM acetyl coenzyme A, and 0.2 mM 5-5′-dithio-bis 2-nitrobenzoic acid (DTNB) was added to

a Tris–HCl buffer (10 mM), pH 7.4, containing 0.2% (v/v) Triton X-100. The reaction was started, after a 10 min preincubation, by the addition of 0.5 mM oxalacetate and the initial rate was measured following the reduction of DTNB at 412–360 nm ($\Delta\varepsilon = 13.6\,mM^{-1}\,cm^{-1}$).

Protein concentration was determined according to Bradford method, using BSA as standard.

Western blot analysis of mitochondrial proteins

For western blots, equal amounts of total cellular proteins (10–20 μg) were separated on a 13% SDS–polyacrylamide gel and transferred onto nitrocellulose membrane. Membranes were then blocked with 5% nonfat milk in 0.1% TBS–Tween-20 and probed with specific antibodies against mitochondrial-encoded subunit I (COXI gene, Molecular Probes, Eugene, OR, USA) and 20 kDa subunit (MTND6 gene, Molecular Probes) and against nuclear-encoded subunit IV (COXIV, Molecular Probes) and 39 kDa subunit (NDUFA9 gene, Molecular Probes) of respiratory complex I and complex IV, respectively. Membranes were also probed with specific antibodies against actin (from Sigma) utilized as loading control. Membranes were finally incubated with HRP-conjugated secondary antibodies and developed with a chemiluminescent reagent (NEN). The bands were quantified with a VersaDoc 1000 Imaging System using the Quantity One software (Bio-Rad Laboratories, Hercules, CA, USA).

Isolation of genomic DNA

Genomic DNA was isolated from cells by a proteinase K/SDS treatment and phenol/chloroform extraction according to standard procedures (14). Total DNA was extracted from cell cultures by IsoQuick Nucleic Acid Extraction kit (ORCA Research, Inc., Bothell, WA, USA) according to manufacturer's procedures.

PCR amplification and sequencing of the mtDNA

Oligonucleotides used for PCR amplification and mtDNA sequencing were named and numbered according to the original published human mtDNA sequence (15). Extension of the number by *-For* or *-Rev* indicates the 5′–3′ direction of the oligonucleotide according to the published sequence. In detail, the primer pairs 15501-For/7608-Rev and 6203-For/16492-Rev were used to amplify the entire human genome in two fragments using the Taq Polymerase gold amplification kit and protocol (Applied Biosystems, Foster City, CA, USA). Sequencing of the purified DNA fragments was carried out utilizing the ABI BigDye Terminator sequencing kit in conjunction with the ABI 310 DNA sequencer and the following primers: 534-For (nts 534–553); 679-Rev (nts 679–658); 1319-For (nts 1319–1336); 1696-Rev (nts 1696–1677); 1749-For (nts 1749–1765); 2162-For (nts 2162–2182); 2525-For (nts 2525–2541); 3345-Rev (nts 3345–3325); 3654-For (nts 3654–3674); 3717-Rev (nts 3717–3701); 4508-Rev (nts 4508–4489); 4828-For (nts 4828–4847); 4966-Rev (nts 4966–4951); 5312-For (nts 5312–5331); 5720-For (nts 5720–5738); 5971-For (nts 5971–5988); 6203-For (nts 6203–6224); 6301-For (nts 6301–6321); 6790-For (nts 6790–6810); 7392-For (nts 7392–7411); 7608-Rev (nts 7608–7588); 7707-For (nts 7707–7723); 8150-For (nts 8150–8166); 8557-For (nts 8557–8574); 9026-For (nts 9026–9042); 9500-For (nts 9500–9520); 9911-For (nts 9911–9932); 10126-For (nts 10126–10146); 10712-For (nts 10712–10728); 11141-For (nts 11141–11158); 11673-For (nts 11673–11692); 11979-For (nts 11979–11995); 12376-For (nts 12376–12394); 12861-For (nts 12861–12877); 13197-For (nts 13197–13213); 13595-For (nts 13595–13611); 14000-For (nts 14000–14023); 14407-For (nts 14407–14424); 15243-For (nts 15243–15259); 15360-Rev (nts 15360–15343); 15501-For (nts 15501–15522); 16162-Rev (nts 16162–16140); 16492-Rev (nts 16492–16471); 16493-For (nts 16493–16514); 16547-Rev (nts 16547–16527)

T414G detection

Primers For1-20 and Rev690-711 amplified a 711-bp fragment of the D-loop region. Amplification parameters were: 5 min at 94°C for the first cycle, denaturation at 94°C for 30 s, annealing at 56°C for 30 s, extension at 72°C for 45 s for the subsequent 28 cycles and a final extension at 72°C for 10 min. PCR products were analyzed by SfaNI digestion for 3 h at 37°C. All digested products were separated by electrophoresis using a 2.5% agarose gel and visualized under ultraviolet light after staining with ethidium bromide.

Identification and quantification of point mutations by mispairing PCR

To analyze the T1843C, A1940G and A2623G point mutations in the 16S rRNA gene by mispairing PCR, part of the mitochondrial ribosomal gene was amplified by 1486-For (cccgtcaccctcctcaagtatacttca) and 3015-Rev (ccatcgggatgtcctgatccaaca). The amplified fragment served as target for the nested amplifications with the following primer sets. Characterizations of nucleotides 1843 and 1940 were carried out by nested amplification utilizing the primer combinations wt/mut1819-For and wtA1960-Rev, wt/mut1819-For and mutG1960-Rev; analysis of position 2623 was realized by amplifying fragments utilizing the primer combinations 2559-For and wtA2650-Rev and 2559-For and mutG2650-Rev.

The following primers were utilized during mispairing PCR amplification (bold nucleotides indicate modified nucleotides that introduce a partial cleavage sequence that is completed either by the following wild-type or mutant sequence):

wt/mut1819-For: (aagcataatatagcaaggactaaccc**G**ta)
wtA1960-Rev: (actattttgctacatagacgggtg**A**gc)
mutG1960-Rev: (actattttgctacatagacgggtg**G**gc)
2559-For: (catgttcggccgcggtaccctaa)
wtA2650-Rev: (aaccctcgtggagccattcatac**C**gg)
mutG2650-Rev: (aaccctcgtggagccattcatac**G**gg)

Analysis of position 1843 was carried out by cleaving the amplified fragment either with XmiI (cleaves the mispairing PCR-modified wild-type mtDNA) or RsaI (cleaves the mispairing PCR-modified mutated mtDNA). Characterization of position 1940 was performed by cleaving the amplified fragment by SacI (cleaves the mispairing PCR-modified wild-type mtDNA) or Bsp120I (cleaves the mispairing PCR-modified mutant mtDNA). Position 2623

was characterized by cleaving the amplified fragments either with BshTI (cleaves the mispairing PCR-modified wild-type mtDNA) or Bsp120I (cleaves the mispairing PCR-modified mutant mtDNA). The cleaved products were visualized by ethidium bromide staining.

The images shown in this article are ethidium bromide stains that do not necessarily display accurately the quantitative yields.

Cloning and sequencing

Primers corresponding to nucleotide positions (nt, 5′–3′, according to Cambridge sequence (15)) For1549–1570 and Rev3359–3380 amplified a 1831-bp coding region spanning the entire MT-RNR2 gene. All PCR fragments were obtained with the Platinum TAQ DNA Polymerase High Fidelity. Amplification parameters were: 2 min at 95°C for the first cycle, denaturation at 94°C for 30 s, annealing at 55°C for 30 s, extension at 68°C for 2 min for the subsequent 27 cycles and a final extension at 72°C for 10 min. PCR fragments were subcloned into a suitable plasmid using TOPO TA cloning kit (Invitrogen, Carlsbad, CA, USA); several independent clones were analyzed, randomly isolated from each single PCR fragment. Cloned mtDNA molecules were used as template in a second round of PCR using commercial primers T3 and T7. PCR products were purified using ExoSAP-IT treatment (Amersham Biosciences, Buckinghamshire, UK) and dispensed in 96-well plates for sequencing with an automated sequencer 3100 (Applied Biosystem) and analyzed with SeqScape Sequence Analysis software. The mutational burden for a given sample was calculated as the number of mutations (defined as discrepancies with the Cambridge reference sequence) found in multiple clones divided by the total number of sequenced bases.

Graphical representation of human mitochondrial LSU RNA

The secondary structure model of human mitochondrial 16S rRNA was derived from entry V00710 of the ribosomal database (16) with *Escherichia coli* 23S rRNA as a template and visualized with RnaViz2 (17). The structure was manually refined and some minor changes were included in the H2 and H4 helices. Numbering of 16S rRNA nucleotides and helical regions is according to the database alignment; structural domains are indicated by roman numbering.

Statistical analysis

Data are expressed as means ± SD and were statistically analyzed utilizing the Student's *t*-test.

RESULTS

Cybrid cell lines derived from fusion experiments that were carried out between 143B.ρ^0 cells [prepared as described earlier by King and Attardi (18)] and enucleated fibroblasts from a 100-year-old donor. The cell lines were described earlier by Michikawa *et al.* (10). In particular, the AL4.8 and AL4.27 are homoplasmic wild-type at position 414 of the human mitochondrial genome, whereas the AL4.3 and AL4.5 carried the age-associated T414G transversion at a homoplasmic level.

Preliminary screening of the bioenergetic competence of the cell clones was carried out by their ability to grow on galactose selective medium (Table 1). It turned out that all cell lines were capable of growing on galactose, besides clone AL4.3 (mut). This was confirmed by the analysis of the endogenous respiratory fluxes measured in intact cells. In fact, it is shown in Table 1 that the basal and the maximal dinitrophenol uncoupled respiration rates of the AL4.3 cells were significantly lower as compared with all the other cell lines. No significant differences were observed among all other cell lines. Surprisingly, even the homoplasmic mutant AL4.5 cells, although coming from the same mitochondrial donor, displayed full bioenergetic competence. Furthermore, we also examined an additional homoplasmic mutant T414G cybrid cell line (AC1.2) that was derived from a different mitochondrial donor (age of 98 years) and also showed full bioenergetic competence. This led us to the conclusion that the T414G mutation is not *per se* responsible for the diminished respiration rate.

In order to identify the enzymatic defect possibly associated with the respiratory deficiencies of the AL4.3 cell line, the enzyme activities of the mitochondrial respiratory complexes were measured spectrophotometrically.

As shown in Table 2, the AL4.8 (wt) cell line does not show any significant difference with the parental cell line 143B.TK$^-$. On the other hand, complex I, complex II + III and complex IV activities of the AL4.3 cell line were decreased by 81, 55 and 62%, respectively, as compared with the AL4.8 cell line. However, complex II activity is not being affected in the AL4.3 cell line.

The above differences were confirmed when normalizing the enzyme activities of the respiratory complexes to mitochondrial matrix marker citrate synthase (data not shown). No significant difference was found when analyzing AL4.5 cells (data not shown), thus confirming no direct linkage between the T414G mutation and the respiratory defects found in the AL4.3 cell line. Nevertheless, the specific decline of the mitochondrial complexes I, II + III and IV that do contain

Table 1. Mitochondrial bioenergetic competence of 143B. TK$^-$ and transmitochondrial cell lines

Cell Line (genotype)	Growth in galactose	Endogenous respiration [nmol O_2/min/$mg_{prot.}$]	DNP-uncoupled respiration [nmol O_2/min/$mg_{prot.}$]
143B.TK$^-$ (414T)	+	9.9 ± 0.4	16.8 ± 2.0
AL4.8 (414T)	+	8.7 ± 1.0	14.2 ± 2.3
AL4.27 (414T)	+	9.1 ± 1.1	14.9 ± 0.6
AL4.3 (T414G)	−	2.5 ± 0.3*	3.4 ± 0.6**
AL4.5 (T414G)	+	9.7 ± 1.1	15.4 ± 1.7

The transmitochondrial cell lines derived from fusion experiments between a 100 year-old fibroblast donor and mtDNA-less acceptor cell-line (143B.TK$^-$ρ206). Cells were tested for their ability (+/−) to grow on galactose selective medium. The values of the respiration rates represent the mean values ± SD from 2–4 independent experiments. *$P < 0.01$ and **$P < 0.05$; AL4.3 versus AL4.8 (see Materials and methods section for experimental details).

mitochondrial encoded subunits and the absence of any defect in the nuclear encoded complex II, pinpoints to the possibility of the existence of other yet unknown mtDNA variants in the AL4.3 cell line.

This led us to sequence the entire mitochondrial genome of the AL4.8 and AL4.3 cybrid cell lines. Apart from the difference at position 414 (T in the AL4.8 and G in AL4.3), 21 homoplasmic single base replacements were detected in both cell lines when compared to the Sanger sequence (15). Three mutations were located in the D-loop, one in the 12S ribosomal RNA gene and 17 in protein coding regions (see Supplementary Material I for a detailed list of the mitochondrial genotype).

Surprisingly, the AL4.3 cells displayed three additional heteroplasmic mutations all clustered within the 16S rRNA gene, namely T1843C, A1940G and A2623G (Figure 1). These mutations were neither detectable in the AL4.8 cell line (Figure 1), the AL4.5 and the AL4.27 cell line, nor in the original DNA extract of the donor fibroblasts (data not shown). Interestingly, the A2623G mutation cosegregated in homoplasmic form together with the T414G mutation in the above mentioned cybrid (AC1.2) deriving from a different mitochondrial donor. Also, in this case, the bioenergetic competence of the AC1.2 cell line excluded a direct impact of the A2623G mutation on the mitochondrial functionality.

To quantify the heteroplasmic states of the 16S rRNA mutations, we decided to develop a mispairing PCR test.

Table 2. Enzyme activity of mitochondrial respiratory complexes from 143B.TK$^-$, AL4.8 and AL4.3 cybrid cells

Cell line	I	II	II + III	IV
143B.TK$^-$ [nmoles/mg/min]	14.5 ± 23	46.2 ± 11.8	33.0 ± 9.8	24.7 ± 7.4
AL4.8 [% of 143B.TK$^-$]	113 ± 48	117 ± 34	119 ± 44	116 ± 52
AL4.3 [% of AL4.8]	21 ± 4*	104 ± 13	53 ± 22*	44 ± 19*

The values represent the mean values ± SD from 3–9 independent experiments. The enzyme activities of the parental 143B cell line are expressed as nanomoles per milligram per minute. The enzyme activities of the AL4.8 and AL4.3 cybrid cell lines are expressed as percentage values of the 143B and AL4.8 cell lines, respectively. *$P < 0.0001$; AL4.3 versus AL4.8 (see Materials and methods section for experimental details).

In this context, a partial region of the 16S rRNA gene was amplified that encompassed the positions of all three point mutations (see Materials and methods section for details). The amplified product served as target for nested PCRs, so that upon RFLP analysis, mutated and wild-type mtDNA could be distinguished by gel electrophoresis (Figure 2) and quantified accordingly. The heteroplasmic mutation levels obtained as the mean value of the quantification of the cleaved fragments were of 54, 64 and 54% for the T1843C, A1940G and A2623G, respectively. These values were in agreement with the relative values of the wild-type and mutant peaks of the electropherograms displayed in Figure 1.

Due to the limitations of the direct sequencing (secondary DNA structure), as well as of the mispairing PCR approach ('heteroduplex formation') and RFLP analysis (partial enzyme cleavage) in quantifying heteroplasmic mtDNA mutations, we decided to apply the same cloning and sequencing technique originally used for the T414G mutations (6). This technique additionally allowed us to position the three mutations on the mitochondrial DNA at a molecular level. As shown in Table 3, the T1843C and A1940G showed a striking cosegregation as opposed to the A2623G mutation thus accounting for at least three distinct mitochondrial genome types just in relation to the three above mentioned 16S rRNA mutations. On 36 analyzed, genetically independent clones, 61% carried both the T1843C and A1940G mutations, while 33% carried only the A2623G mutation. One clone carried only wild-type DNA in respect to 1843, 1940 and 2623, while another one carried only the A1940G mutation. A similar analysis was carried out on AL4.8 DNA and confirmed exclusively wild-type sequence at positions 1843, 1940 and 2623 (data not shown). Additionally, a similar amount of randomly distributed point mutations was found at a low percentage (1–2/36 clones) within the analyzed fragment in both the AL4.8 and AL4.3 cybrids, with the exception of T1975C (3/36 clones) in the AL4.3 DNA (see Supplementary Material II for a detailed genotype list of the 16S rRNA containing clones).

To distinguish which of the three 16S rRNA mutations may account for the bioenergetic deficiencies observed in

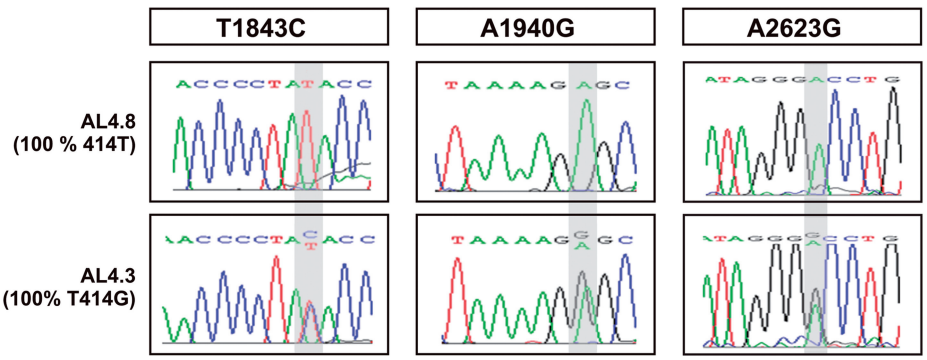

Figure 1. Sequence analyses of the mitochondrial 16S rRNA genes. Displayed are the electropherograms related to the 1843, 1940 and 2623 positions in the 16S rRNA genes of the AL4.8 and AL4.3 cells. The shaded areas highlight the homoplasmic and heteroplasmic peaks of wild-type and mutated mtDNAs, respectively.

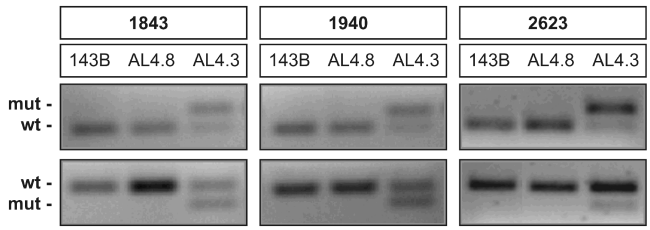

Figure 2. Mispairing PCR and RFLP analyses of heteroplasmic point mutations in the mitochondrial 16S rRNA gene. The 1843, 1940 and 2623 positions were analyzed by RFLP analyses as described under Materials and methods section. XmiI, SacI and BshTI restriction enzymes were used to cleave the mispairing PCR products carrying the wild-type genotype at positions 1843, 1940 and 2623, respectively (upper panels). RsaI and Bsp120I restriction enzymes were used to cleave the mispairing PCR products carrying the mutant genotype at positions 1843 and 1940 or 2623, respectively (lower panels). The displayed ethidium bromide stained gels (upper and lower panels) refer to representative experiments.

Table 3. Analyses of the 16S rRNA gene mutations by cloning-sequencing approach in AL4.3 cells

AL4.3	Mitochondrial genotypes		
	T1843C	A1940G	A2623G
1			+
2	+	+	
3	+	+	
4	+	+	
5	+	+	
6	+	+	
7	+	+	
8			+
9			+
10			
11	+	+	
12	+	+	
13			+
14			+
15	+	+	
16			+
17	+	+	
18	+	+	
19	+	+	
20	+	+	
21	+	+	
22			+
23		+	
24	+	+	
25	+	+	
26			+
27			+
28	+	+	
29	+	+	
30			+
31			+
32	+	+	
33	+	+	
34	+	+	
35			+
36	+	+	

The 36 *E. coli* clones carried the mtDNA fragment encompassing nucleotides 1671–3228 of the 16S rRNA gene derived from AL4.3 cells (see Materials and methods Section as well Supplementary Material II for further details and complete sequences).

Table 4. Analyses of the 16S rRNA gene mutations by cloning-sequencing approach in galactose selected AL4.3 cells

AL4.3	Mitochondrial genotypes		
Gal–select	T1843C	A1940G	A2623G
1			+
2	+	+	
3			
4	+	+	
5		+	
6	+		+
7	+		
8	+		
9			+
10			+
11			+
12			+
13	+	+	
14			+
15			+
16			+
17	+	+	
18	+	+	
19	+	+	
20	+	+	
21			+
22			+
23			+
24	+	+	
25			+
26			+
27	+	+	
28	+	+	
29	+	+	
30	+	+	
31			+
32	+	+	
33			+
34			+
35	+	+	
36	+	+	

The 36 *E. coli* clones carried the mtDNA fragment encompassing nucleotides 1671–3228 of the 16S rRNA gene derived from galactose-selected AL4.3 cells (see Materials and methods section as well Supplementary Material II for further details and complete sequences).

the AL4.3 cells, we decided to study the genetic drift of AL4.3 cell line upon selective growth conditions. When cells were selected on galactose medium under otherwise identical conditions (Table 4), interestingly the T1843C and A1940G levels were selectively diminished (50 and 44%, respectively), while A2623G level increased up to 47%. These results confirmed the T1843C and A1940G mutations as those most likely being responsible of the mitochondrial defects. Interestingly, the T1975C mutation level was also increased after galactose selection (5/36 clones).

In the light of the clustered appearance of the three mutations in the 16S rRNA gene, we measured the protein expression of mitochondrial- and nuclear-encoded subunits of respiratory complex I and complex IV. As shown in Figure 3, the protein level of nuclear-encoded subunit IV and 39 kDa subunit of complex IV and complex I, respectively, was similar in AL4.8 and AL4.3 total cell lysates. On the other hand, the level of the mitochondrial-encoded catalytic subunit I of respiratory complex IV of AL4.3 cells

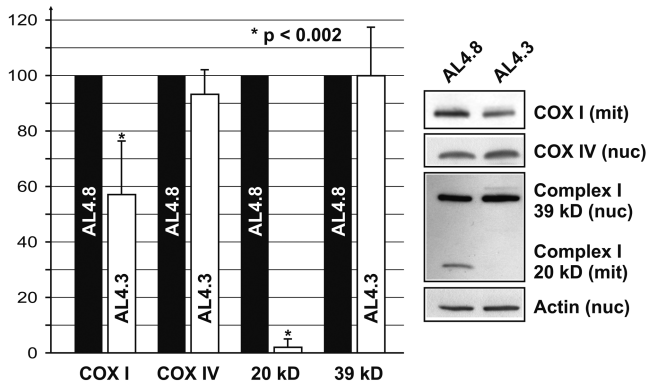

Figure 3. Expression level of nuclear- and mitochondrial-encoded subunits of respiratory complex I and complex IV. Nuclear- (nuc) and mitochondrial- (mit)encoded complex I and complex IV subunit levels in AL4.3 cells (white bars) were normalized to actin and expressed as percent of the AL4.8 control cells (black bars = 100%). The western blot analysis was carried out on total cell lysates. The values represent the average of four independent determinations ± SD.

was significantly reduced by 43% as compared with AL4.8 cells, with this change being in good agreement with the above described reduction in complex IV activity (Table 2). Furthermore, the mitochondrial-encoded 20 kDa subunit of respiratory complex I was barely detectable in AL4.3 cells. These results confirmed the direct and specific impact of the 16S rRNA mutations on mitochondrial protein synthesis machinery.

DISCUSSION

The open controversy about a possible involvement of mtDNA variations in the aging process makes it necessary to associate functional data to genetic association studies. The discovery of the age-associated accumulation of the T414G mutation in human fibroblast mtDNA in 1999 (6) shifted the attention from simple DNA rearrangements to the more complex single and multiple base replacements. Consequently, the tissue specificity of certain point mutations was genetically linked to the general aging process (19) as well as to age-associated neurodegenerative disorders (20). Some of these mutations have been shown to affect mtDNA transcription and/or replication (20,21), but their impact on the bioenergetic functionality of mitochondria has not yet been investigated. Furthermore, the simultaneous occurrence of different mutations makes it difficult to assign specific effects to single mutations, while giving more importance to their synergy hence to the mitochondrial haplotype (22,23). Even the earliest developmental processes seem to attribute certain aspects of aging, since the T414G transversion accumulates in an age-dependent manner in human oocytes (24).

Cybrid cell lines have long been used in the analysis of mutant mtDNA on a neutral nuclear background so that biochemical and enzymatic analysis could be carried out. The rationale behind the use of the transmitochondrial cell lines was mainly based on the assumption that in these cells the possibility of differently expressed nuclear isoforms as well as the impact of different nuclear haplotypes on the overall cellular phenotype should have been avoided. Therefore, we have utilized transmitochondrial cybrids generated by the fusion of cytoplasts from aged individuals with mtDNA-depleted 143B.TK$^-$ (ρ^0 cells), thus carrying either the 414T (wild-type) or 414G (mutant) mtDNA genotype. The first outcome of this analysis excludes a direct impact of the T414G mutation onto the mitochondrial bioenergetic efficiency and capacity. In fact, two cybrid cell lines homoplasmic for the T414G mutation showed a full bioenergetic competence. However, the existence of a third homoplasmic T414G cybrid cell line presenting with a deficient bioenergetic phenotype strongly suggested the possibility of additional mtDNA variants. Indeed, we found three additional ribosomal RNA mutations, two of which, i.e. T1843C and A1940G were recorded for the first time at MitoMap database (25). The third mutation (A2623G) was previously reported as to be a polymorphic site (26) although it was not functionally characterized. Our results clearly rule out the A2623G mutation produces any detectable bioenergetic defect since the coexistence of this mutation at a homoplasmic level together with the T414G mutation has been found in a fully respiratory competent transmitochondrial cybrid cell line. This conclusion is strengthened by the finding that the heteroplasmic level of this mutation in galactose selected cells is increased.

Our results lead us to propose that the T1843C and the A1940G mutations are the cause of the observed bioenergetic deficiency. The underlying molecular mechanism is most likely linked to the malfunctioning translational system of mitochondria, since the 16S rRNA is an integral member of the mitochondrial protein synthesis machinery.

As shown in Figure 4, the mutations relevant for the bioenergetic deficiency are not located in close proximity to the catalytic center of the rRNA, which is mainly formed by the central loop of domain VI (27). Instead, they are located in the 5′ part of the RNA. The role of the A1940G mutation (A270G in the RNA) is readily explained, because the change leads to formation of a G•U wobble pair instead of a regular A–U base pair, and thus will destabilize helix D8 in domain II. Although this helix is not directly linked to the catalytic region, a tertiary interaction between A323 in Loop D10 to C767 in the E16–E4 junction (green line in Figure 4) will bring this whole structure in close proximity to the peptidyl transferase center and may thus influence the overall stability of this domain.

The defect caused by the T1843C mutation (U173C in the RNA) is not as straightforward to explain, because domain I in mitochondrial 16S rRNA is much less structured than the corresponding part of bacterial 23S rRNA. Whereas the latter is forming a highly ordered stem-loop arrangement and is linked to the 3′- end of the RNA by a regular helical stem, only some small isolated stem-loop structures are present in the mitochondrial RNA, and no extended pairing to the 3′-end is possible. Even a manual search for alternative secondary structures in the region did not reveal any possible structural stabilization within this region close to the 5′-end of 16S rRNA.

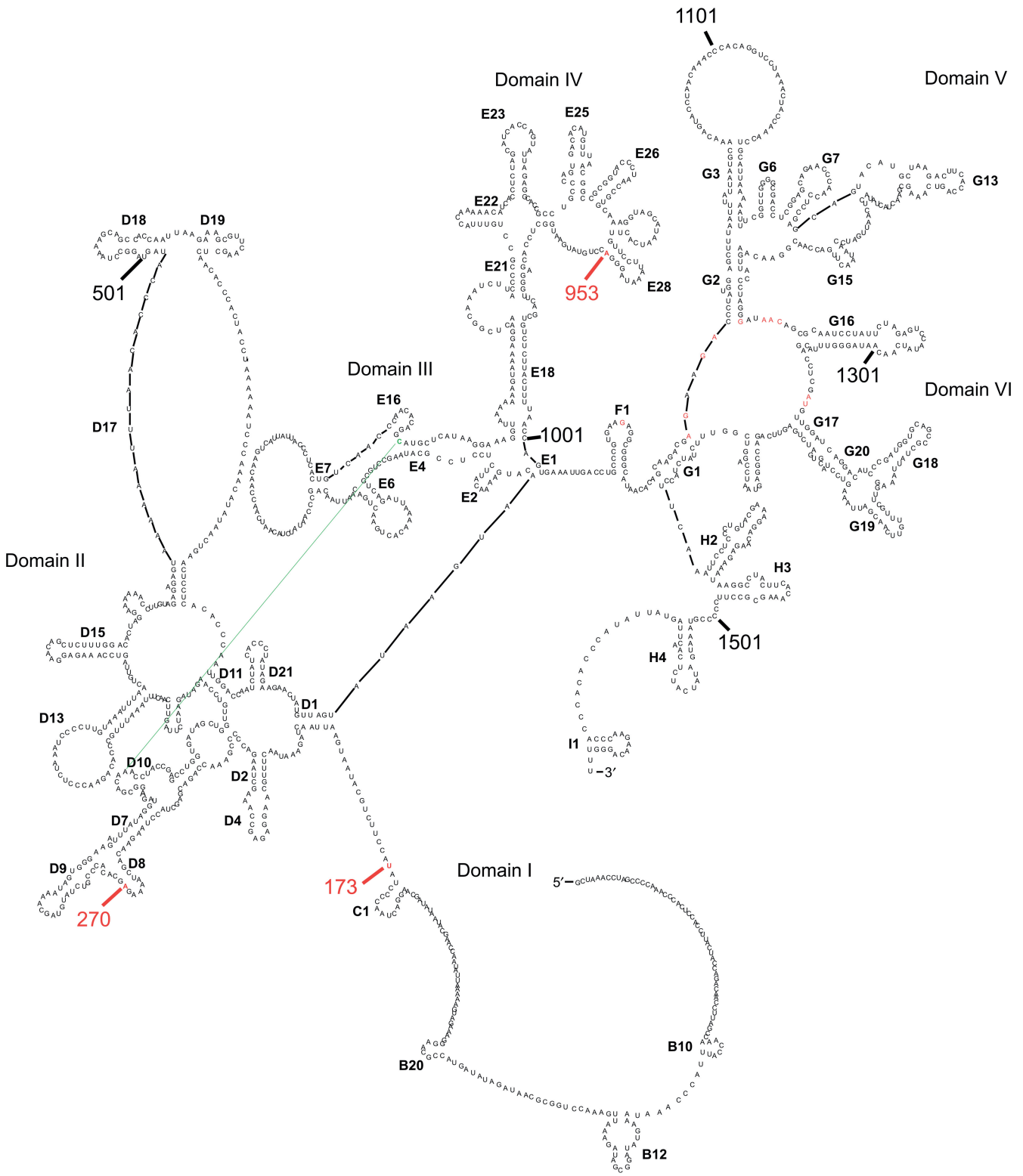

Figure 4. Predicted secondary structure of the mitochondrial 16S rRNA. The nucleotides in the peptidyl transferase region (the multi-branched loop connecting helices G1–G2–G16–G17), which are relevant for catalytic activity or chloramphenicol binding in bacterial 23S rRNAs are highlighted in red. The mutations in mitochondrial 16S rRNA are also highlighted in red and their position within the rRNA is additionally indicated by red numbers. Base numbering is according to the Ribosomal Database: position 173 corresponds to T1843C; position 270 to A1940G, and position 953 to A2623G, respectively. The long-range interaction between C767 and A323 is depicted by a thin green line. For clarity, base and helix numbering is not contiguous.

However, an effect on mitochondrial 16S rRNA modification, stability and/or folding as well as an effect on ribosome assembly due to the interaction of nucleic acid and protein subunits needs to be investigated. The functional effect of the mutations on mitochondrial translation is clearly demonstrated by the specific decline of mitochondrial-encoded subunits of respiratory complex I and IV observed by western blot analysis on total cell lysates of AL4.3 cells, when compared to AL4.8 control cells.

As stressed elsewhere (28), the coexistence of different mutations in the same gene makes it difficult to assign a specific function to each position unless clones carrying only one of these mutations can be selected, as in the case of the A2623G mutation in our study.

The discovery of three clustered mutations in the 16S rRNA gene cosegregating together with the T414G mutation offered us the possibility both to investigate the phenotypic effect of novel mtDNA variants as well as to suggest a different mechanism by which the age-associated T414G mutation could lead to the accumulation of additional mtDNA mutations (generator for mtDNA alterations).

The striking observation that the T1843C and the A1940G mutation appeared at a heteroplasmic state may account for their recent occurrence in relation to the homoplasmic presence of the T414G mutation. Even more, the cloning and sequencing data clearly show that T1843C and the A1940G appear on the same DNA molecules as opposed to the A2623G mutation. If mutations in the ribosomal gene region alter the looping mechanism shown to occur during rRNA transcription (29), the efficiency of the mtDNA replication cycle could be affected as well. This could possibly explain the recently reported linkage between a common photoaging-associated mtDNA deletion and the T414G mutation (30).

Overall, this highlights the complex heterogeneity and the dramatic instability of the mitochondrial genome during tissue culture conditions (23). This is worsened by the high variability of the osteosarcoma karyotype of the 143B.TK$^-$ acceptor cell line (P.S., unpublished data). The present observation also underlines the need of a continuous monitoring of mtDNA fidelity when utilizing transmitochondial cybrids, especially if patient's diagnostics has to rely exclusively on results obtained by this valuable and so far irreplaceable technique.

SUPPLEMENTARY DATA

Supplementary Data are available at NAR Online.

ACKNOWLEDGEMENTS

G.V., in agreement with all the authors, wishes to dedicate this article to the memory of his recently deceased 'maestro' Giuseppe Attardi who kindly provided all the cell lines described herein. The authors are grateful to Angela Mühlberg for preparing the article.

FUNDING

National Research Project (PRIN 2003 n° 2003064310_002 and PRIN 2006 n° 2006069034_004 to G.V.) of the Italian Ministry for the University (MIUR); the Sächsische Ministerium für Wissenschaft und Kunst SMWK. Funding for open access charge: Genaxxon Bioscience GmbH, Biberach, Germany.

Conflict of interest statement. None declared.

REFERENCES

1. Crouch,P.J., Cimdins,K., Duce,J.A., Bush,A.I. and Trounce,I.A. (2007) Mitochondria in aging and Alzheimer's disease. *Rejuvenation. Res.*, **10**, 349–357.
2. Wallace,D.C. (2005) A mitochondrial paradigm of metabolic and degenerative diseases, aging, and cancer: a dawn for evolutionary medicine. *Annu. Rev. Genet.*, **39**, 359–407.
3. Attardi,G. (2002) Role of mitochondrial DNA in human aging. *Mitochondrion.*, **2**, 27–37.
4. Kraytsberg,Y., Kudryavtseva,E., McKee,A.C., Geula,C., Kowall,N.W. and Khrapko,K. (2006) Mitochondrial DNA deletions are abundant and cause functional impairment in aged human substantia nigra neurons. *Nat. Genet.*, **38**, 518–520.
5. Bender,A., Krishnan,K.J., Morris,C.M., Taylor,G.A., Reeve,A.K., Perry,R.H., Jaros,E., Hersheson,J.S., Betts,J., Klopstock,T. *et al.* (2006) High levels of mitochondrial DNA deletions in substantia nigra neurons in aging and Parkinson disease. *Nat. Genet.*, **38**, 515–517.
6. Michikawa,Y., Mazzucchelli,F., Bresolin,N., Scarlato,G. and Attardi,G. (1999) Aging-dependent large accumulation of point mutations in the human mtDNA control region for replication. *Science*, **286**, 774–779.
7. Trifunovic,A., Wredenberg,A., Falkenberg,M., Spelbrink,J.N., Rovio,A.T., Bruder,C.E., Bohlooly,Y., Gidlof,S., Oldfors,A., Wibom,R. *et al.* (2004) Premature ageing in mice expressing defective mitochondrial DNA polymerase. *Nature*, **429**, 417–423.
8. Vermulst,M., Bielas,J.H., Kujoth,G.C., Ladiges,W.C., Rabinovitch,P.S., Prolla,T.A. and Loeb,L.A. (2007) Mitochondrial point mutations do not limit the natural lifespan of mice. *Nat. Genet.*, **39**, 540–543.
9. Khrapko,K. and Vijg,J. (2007) Mitochondrial DNA mutations and aging: a case closed? *Nat. Genet.*, **39**, 445–446.
10. Michikawa,Y., Laderman,K., Richter,K. and Attardi,G. (1999) Role of nuclear background and in vivo environment in variable segregation behavior of the aging-dependent T414G mutation at critical control site for human fibroblast mtDNA replication. *Somat. Cell Mol. Genet.*, **25**, 333–342.
11. Villani,G. and Attardi,G. (2007) Polarographic assays of respiratory chain complex activity. *Methods Cell Biol.*, **80**, 121–133.
12. Villani,G. and Attardi,G. (1997) In vivo control of respiration by cytochrome c oxidase in wild-type and mitochondrial DNA mutation-carrying human cells. *Proc. Natl Acad. Sci. USA*, **94**, 1166–1171.
13. Sgobbo,P., Pacelli,C., Grattagliano,I., Villani,G. and Cocco,T. (2007) Carvedilol inhibits mitochondrial complex I and induces resistance to H_2O_2 -mediated oxidative insult in H9C2 myocardial cells. *Biochim. Biophys. Acta*, **1767**, 222–232.
14. Shoffner,J.M., Lott,M.T., Lezza,A.M., Seibel,P., Ballinger,S.W. and Wallace,D.C. (1990) Myoclonic epilepsy and ragged-red fiber disease (MERRF) is associated with a mitochondrial DNA tRNA(Lys) mutation. *Cell*, **61**, 931–937.
15. Anderson,S., Bankier,A.T., Barrell,B.G., de Bruijn,M.H., Coulson,A.R., Drouin,J., Eperon,I.C., Nierlich,D.P., Roe,B.A., Sanger,F. *et al.* (1981) Sequence and organization of the human mitochondrial genome. *Nature*, **290**, 457–465.
16. Wuyts,J., Perriere,G. and van de Peer,Y. (2004) The European ribosomal RNA database. *Nucleic Acids Res.*, **32**, D101–D103.
17. De Rijk,P., Wuyts,J. and De Wachter,R. (2003) RnaViz 2: an improved representation of RNA secondary structure. *Bioinformatics*, **19**, 299–300.

18. King,M.P. and Attardi,G. (1989) Human cells lacking mtDNA: repopulation with exogenous mitochondria by complementation. *Science*, **246**, 500–503.
19. Wang,Y., Michikawa,Y., Mallidis,C., Bai,Y., Woodhouse,L., Yarasheski,K.E., Miller,C.A., Askanas,V., Engel,W.K., Bhasin,S. *et al*. (2001) Muscle-specific mutations accumulate with aging in critical human mtDNA control sites for replication. *Proc. Natl Acad. Sci. USA*, **98**, 4022–4027.
20. Coskun,P.E., Beal,M.F. and Wallace,D.C. (2004) Alzheimer's brains harbor somatic mtDNA control-region mutations that suppress mitochondrial transcription and replication. *Proc. Natl Acad. Sci. USA*, **101**, 10726–10731.
21. Zhang,J., sin-Cayuela,J., Fish,J., Michikawa,Y., Bonafe,M., Olivieri,F., Passarino,G., De,B.G., Franceschi,C. and Attardi,G. (2003) Strikingly higher frequency in centenarians and twins of mtDNA mutation causing remodeling of replication origin in leukocytes. *Proc. Natl Acad. Sci. USA*, **100**, 1116–1121.
22. Del Bo,R., Crimi,M., Sciacco,M., Malferrari,G., Bordoni,A., Napoli,L., Prelle,A., Biunno,I., Moggio,M., Bresolin,N. *et al*. (2003) High mutational burden in the mtDNA control region from aged 'muscles: a single-fiber study. *Neurobiol. Aging*, **24**, 829–838.
23. Ballana,E., Govea,N., de Cid,R., Garcia,C., Arribas,C., Rosell,J. and Estivill,X. (2007) Detection of unrecognized low-level mtDNA heteroplasmy may explain the variable phenotypic expressivity of apparently homoplasmic mtDNA mutations. *Hum. Mutat*, **29**, 248–257.
24. Barritt,J.A., Cohen,J. and Brenner,C.A. (2000) Mitochondrial DNA point mutation in human oocytes is associated with maternal age. *Reprod. Biomed. Online*, **1**, 96–100.
25. Ruiz-Pesini,E., Lott,M.T., Procaccio,V., Poole,J.C., Brandon,M.C., Mishmar,D., Yi,C., Kreuziger,J., Baldi,P. and Wallace,D.C. (2007) An enhanced MITOMAP with a global mtDNA mutational phylogeny. *Nucleic Acids Res*., **35**, D823–D828.
26. Rieder,M.J., Taylor,S.L., Tobe,V.O. and Nickerson,D.A. (1998) Automating the identification of DNA variations using quality-based fluorescence re-sequencing: analysis of the human mitochondrial genome. *Nucleic Acids Res*., **26**, 967–973.
27. Schlunzen,F., Zarivach,R., Harms,J., Bashan,A., Tocilj,A., Albrecht,R., Yonath,A. and Franceschi,F. (2001) Structural basis for the interaction of antibiotics with the peptidyl transferase centre in eubacteria. *Nature*, **413**, 814–821.
28. Pye,D., Kyriakouli,D.S., Taylor,G.A., Johnson,R., Elstner,M., Meunier,B., Chrzanowska-Lightowlers,Z.M., Taylor,R.W., Turnbull,D.M. and Lightowlers,R.N. (2006) Production of transmitochondrial cybrids containing naturally occurring pathogenic mtDNA variants. *Nucleic Acids Res*., **34**, e95.
29. Martin,M., Cho,J., Cesare,A.J., Griffith,J.D. and Attardi,G. (2005) Termination factor-mediated DNA loop between termination and initiation sites drives mitochondrial rRNA synthesis. *Cell*, **123**, 1227–1240.
30. Birket,M.J. and Birch-Machin,M.A. (2007) Ultraviolet radiation exposure accelerates the accumulation of the aging-dependent T414G mitochondrial DNA mutation in human skin. *Aging Cell*, **6**, 557–564.